Structure of a WW domain containing fragment of dystrophin in complex with β-dystroglycan

Xin Huang[1,2], Florence Poy[1], Rongguang Zhang[3], Andrzej Joachimiak[3], Marius Sudol[4] and Michael J. Eck[1,2]

[1]Department of Cancer Biology, Dana Farber Cancer Institute, 44 Binney Street, Boston, Massachusetts 02115, USA. [2]Department of Biological Chemistry and Molecular Pharmacology, Harvard Medical School, Boston, Massachusetts 02215, USA. [3]Biosciences Division, Structural Biology Center, Argonne National Laboratory, Argonne, Illinois 60439, USA. [4]Department of Biochemistry and Molecular Biology, Mount Sinai School of Medicine, New York, New York 10029, USA.

Dystrophin and β-dystroglycan are components of the dystrophin–glycoprotein complex (DGC), a multimolecular assembly that spans the cell membrane and links the actin cytoskeleton to the extracellular basal lamina. Defects in the dystrophin gene are the cause of Duchenne and Becker muscular dystrophies. The C-terminal region of dystrophin binds the cytoplasmic tail of β-dystroglycan, in part through the interaction of its WW domain with a proline-rich motif in the tail of β-dystroglycan. Here we report the crystal structure of this portion of dystrophin in complex with the proline-rich binding site in β-dystroglycan. The structure shows that the dystrophin WW domain is embedded in an adjacent helical region that contains two EF-hand-like domains. The β-dystroglycan peptide binds a composite surface formed by the WW domain and one of these EF-hands. Additionally, the structure reveals striking similarities in the mechanisms of proline recognition employed by WW domains and SH3 domains.

Skeletal muscle dystrophin is a 427 kDa molecule that contains an N-terminal actin binding domain, a central rod-like region composed of 26 spectrin repeats and a C-terminal region that interacts with other proteins in the dystrophin–glycoprotein complex (DGC)[1]. In addition to dystrophin, components of the DGC include the sarcoglycans, syntrophins, dystrobrevins, and the transmembrane glycoprotein β-dystroglycan[2,3]. The C-terminal portion of dystrophin and its interactions with other components of the DGC are particularly important for its function; deletions in this region give rise to a severe dystrophic phenotype in which the DGC fails to form[4,5]. Of the protein interactions in the DGC, the dystrophin–β-dystroglycan interaction has been characterized in the greatest detail[6,7]. A proline-rich epitope encompassing the C-terminal 15 residues of β-dystroglycan is both necessary and sufficient for direct association with dystrophin[6]. The fragment of dystrophin required for the interaction spans ~260 residues of its 'cysteine-rich' C-terminal region[6,7]. Based on its primary sequence[1], this fragment has been suggested to contain both a domain resembling a calcium binding EF-hand domain and a WW domain[7], a modular domain of ~40 amino acids that functions as a protein interaction module by recognizing proline-containing motifs in partner proteins[8]. Interestingly, the dystrophin WW domain alone does not bind β-dystroglycan; binding requires the adjacent EF-hand-like sequences in dystrophin[7].

The WW domain is found in proteins of diverse function, including formin binding proteins, the prolyl-isomerase Pin1, Nedd4 ubiquitin ligase, and the Yes kinase-associated protein YAP[8]. At least five distinct binding motifs have been defined for the WW domain[9,10]. For example, both the dystrophin and YAP WW domains recognize a PPxY motif[7,11] (where x represents any

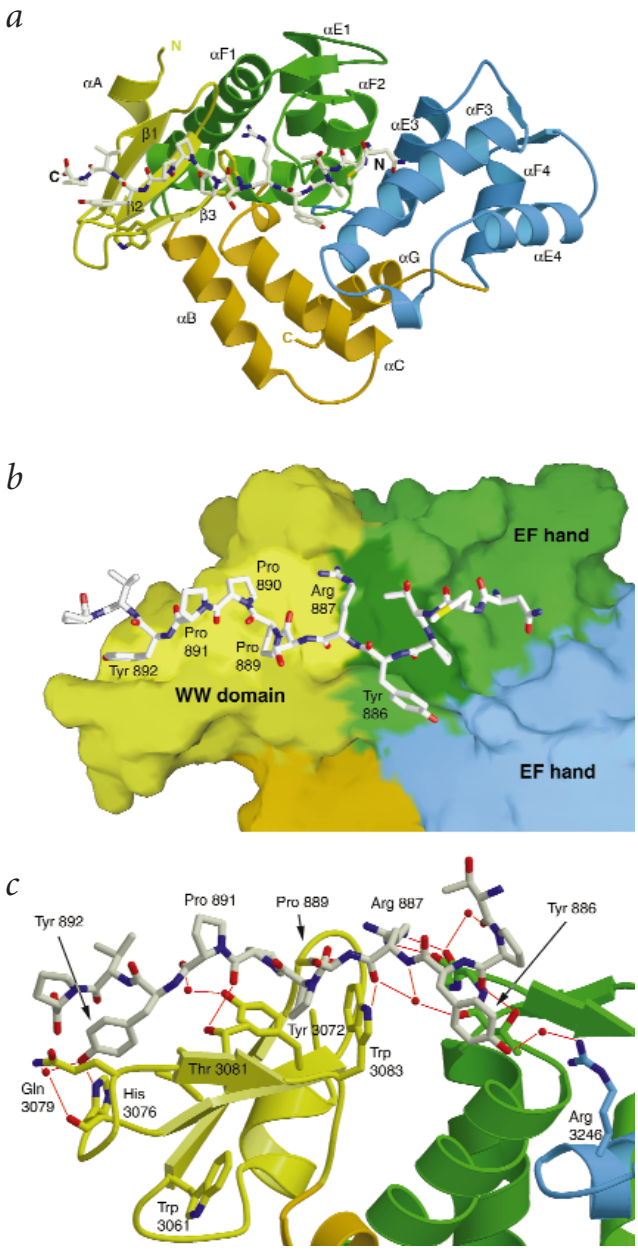

Fig. 1 Structure of the dystrophin–β-dystroglycan complex. ***a***, Ribbon diagram showing the overall organization of the dystroglycan binding region of dystrophin. The WW domain is colored yellow, the first EF-hand domain green, the second EF-hand domain blue, and additional helices gold. The β-dystroglycan peptide (white) extends across the first EF-hand and the WW domain. Elements of secondary structure, the N- and C-termini of the protein, and peptide are labeled. ***b***, Molecular surface of the DBR, colored as in (*a*). The surface of residues in the WW domain and EF-hand that contact the peptide are shaded bright yellow and dark green, respectively, to highlight the binding surface. Peptide residues Pro 889–Tyr 892 constitute the PPxY motif. All Pro residues in the peptide are in the *trans* conformation; those in the PPxY motif form a single turn of polyproline II helix. ***c***, Detailed view of dystrophin–β-dystroglycan recognition. The thin red lines indicate hydrogen bonds. The peptide makes six hydrogen bonds directly to the DBR domain, and an additional six through bridging water molecules (indicated by red spheres).

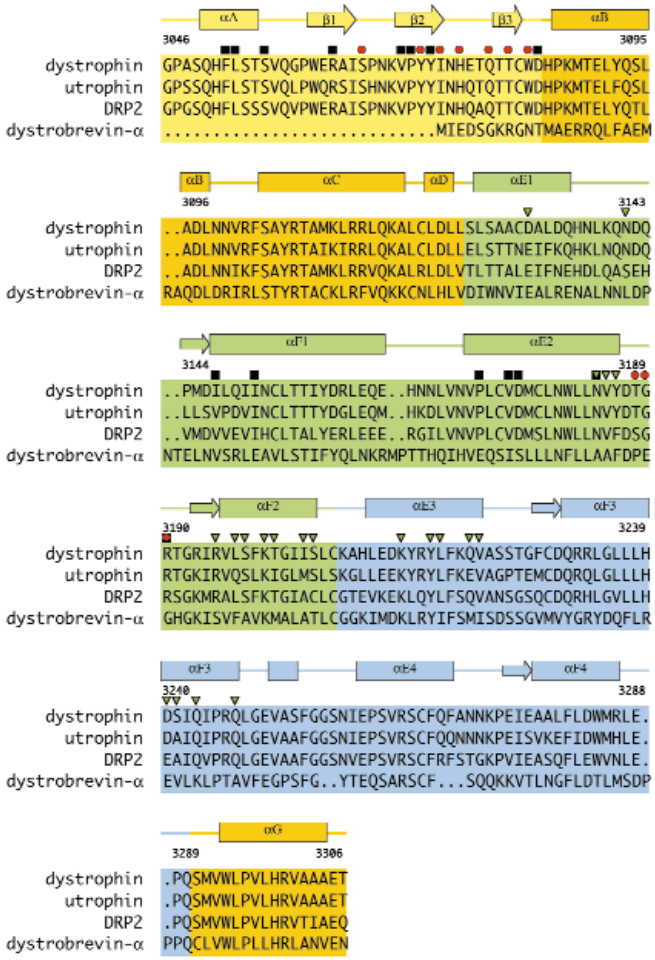

Fig. 2 Aligned sequences of the dystrophin, and dystrophin related proteins utrophin, DRP2, and dystrobrevin-α. Secondary structure elements are shown above the sequence and are colored as in Fig. 1. Red circles mark residues that interact with the β-dystroglycan peptide. Black squares indicate residues that form the interface between the WW domain and the first EF-hand domain. Green triangles denote residues that are at the interface between the first EF-hand domain and the second EF-hand domain.

amino acid), while the formin binding proteins bind a PPLP or PGM motif[12,13]. Additionally, the Pin1 WW domain binds a sequence containing both proline and phosphoserine[14]. Structures of the Pin1 and YAP WW domains show that they consist of a three-stranded β-sheet; the two conserved Trp residues for which the domain is named lie on opposite faces of this sheet[15,16]. An NMR and site-directed mutagenesis study of the YAP WW domain with a PPxY peptide defined the binding site and general orientation of the bound peptide, but did not provide a high resolution view of the complex[16]. Thus, the mechanism of recognition of the PPxY motif is unclear, as is the structural basis for the rather diverse ligand binding properties of other WW domains. To better understand WW domain specificity and the interaction between dystrophin and β-dystroglycan, we determined the X-ray crystal structure of residues 3046–3306 of human dystrophin (referred to here as the dystroglycan-binding region, DBR) alone and in complex with the C-terminal 15 residues of β-dystroglycan (see Table 1 and Methods).

Overall structure and domain organization

The dystrophin DBR is a compact, globular structure consisting of a WW domain, two EF-hand-like domains, and several additional helices that tie the EF-hand and WW domains together (Fig. 1*a*). The ligand binding site on the WW domain, which lies on the 'top' of the three-stranded β-sheet, is exposed on the surface of the molecule. The underside of the WW domain makes extensive contact with the first EF-hand domain, in addition to the N-terminal helix αA. In spite of its extensive interactions with adjacent helical regions, it is very similar in overall structure to the Yap65 WW domain[16] and the Pin1 WW domain[15]. Over 20% of the surface area of the WW domain is buried by contact with neighboring helices; the domain is unlikely to fold properly independent of these interactions. Indeed, the isolated dystrophin WW domain does not bind β-dystroglycan[7]. In contrast, most other WW domains are independently folding units and retain their ligand binding activity in isolation.

Apart from the WW domain, the structure is mostly α-helical. Two helices, αB and αC, follow the WW domain in sequence and connect it to the first of two EF-hand-like domains (Fig. 1*a*). The two EF-hand domains pack side-by-side with their EF-loops facing up. Helices αC and αG cross under the EF-hands, extending the mostly hydrophobic interface between the domains. The EF-hand is a helix-loop-helix motif found in many calcium binding proteins[17]. None of the EF-like motifs in dystrophin contain the canonical pattern of calcium binding residues, and we do not observe bound Ca^{2+} in any of the four EF-loops in our structure. Furthermore, calcium does not affect the affinity of this fragment of dystrophin for β-dystroglycan. Using isothermal titration calorimetry, we measured a dissociation constant of ~40 μM for the binding of β-dystroglycan to the dystrophin DBR fragment both in the absence of calcium and in calcium concentrations as high as 50 mM (data not shown). Divergent EF-hand motifs that do not bind calcium in one or more of the canonical sites have been identified in other protein recognition domains; examples include the Eps15 homology (EH) domain[18] and the phosphotyrosine binding region of c-Cbl[19].

The relative orientation of the WW and EF-hand domains appears to be fixed and relatively inflexible. We observe no significant change in domain orientations in the unliganded structure, and the contacts among the WW and EF-hand domains are extensive and well-conserved among dystrophin homologs (Fig. 2). In addition, we observe the same domain organization in an additional unliganded crystal form with unrelated lattice contacts (data not shown). Thus, we expect that the ligand binding surface in dystrophin is pre-formed in the absence of β-dystroglycan, and that the dystrophin related proteins utrophin and DRP2 will adopt the same quaternary organization. In dystrobrevin-α, which lacks a WW domain, only the interface between the EF-hands appears to be conserved (Fig. 2).

β-Dystroglycan recognition

The β-dystroglycan peptide binds to a continuous surface formed by the WW domain and the first EF-hand-like domain (Fig. 1*b*). The N-terminal portion of the peptide extends across the EF-hand domain; the C-terminal portion, including the PPxY motif, extends across the upper face of the WW domain. The peptide has the sequence KNMT**PYRSPPPY**VPP, corresponding to residues 881–895 of β-dystroglycan. Eight central residues in this peptide (indicated in bold type) bind to a recognition surface formed primarily by the WW domain and also in

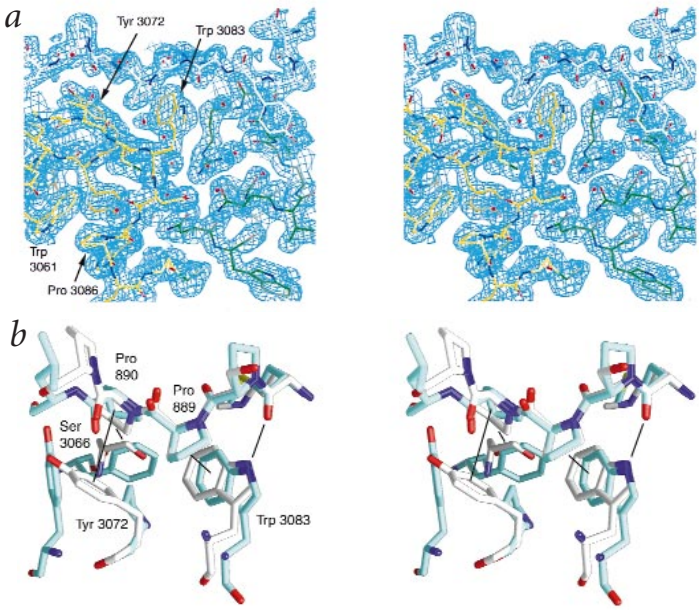

Fig. 3 Stereo views showing the binding mode of Pro residues by the WW domain and comparison to that observed in SH3 domains. ***a***, Electron density map at the interface between the β-dystroglycan peptide and the WW and EF-hand domains. The $2F_o$ - F_c map is contoured at 1.3 σ and was calculated using data to 1.9 Å resolution. The dystrophin domains and the peptide are colored as in Fig. 1. Note the interactions of peptide Pro residues with the 'aromatic cradle' formed by Tyr 3072 and Trp 3083. Residues Trp 3061 and Pro 3086 are highly conserved in WW domains and form the hydrophobic buckle on the underside of the domain. ***b***, Superposition of the dystrophin aromatic cradle with a similar recognition element in the Abl SH3 domain[20]. The superposition was calculated using only the proline-rich peptides (residues 887–890 in the β-dystroglycan peptide, with residues C4–C7 in the Abl SH3–peptide complex). Thin black lines indicate similar hydrogen bond and hydrophobic interactions. Note that the geometry of interaction with the Trp residue is essentially identical in the two structures, including the contact of the Pro with the Trp ring, and the hydrogen bond to the Trp from the carbonyl group of the 'P-2' residue (the residue preceeding the first proline by two positions). The second Pro residue (Pro 890 in β-dystroglycan) makes a van der Waals contact to Ser 3066 that is similar to that made to a Phe ring in the Abl structure. The interaction of Pro 890 with the surface of Tyr 3072 is more divergent; the corresponding surface is formed by a Pro and a Tyr in the SH3 domain. Both SH3 and WW domains have been shown to recognize non-natural N-substituted amino acids (in addition to Pro) at particular positions[33]; the site occupied by Pro 890 is such a position, and it would likely accommodate small hydrophobic N-substituted residues.

part by the first EF-hand domain. Most of the peptide backbone is in an extended conformation, but the three consecutive proline residues form a single turn of polyproline type II (PPII) helix. The PPPY sequence in the peptide forms the core of the interaction. The first two prolines in this motif (residues 889 and 890) insert into a concave hydrophobic surface formed by Tyr 3072 and Trp 3083 in the WW domain. In this 'aromatic cradle', Pro 889 stacks against Trp 3083 and Pro 890 stacks against Tyr 3072 (Figs 1*c*, 3). The carbonyl oxygen of Arg 887 forms a hydrogen bond with the indole nitrogen of Trp 3083 in the WW domain. The tyrosine in the PPPY motif (Tyr 892 in β-dystroglycan) is accommodated in a shallow hydrophobic pocket formed by Ile 3074, Gln 3079 and His 3076 of the dystrophin WW domain. Its hydroxyl group hydrogen bonds with His 3076 (Fig. 1*c*). In the first EF-hand, two main chain carbonyl groups in the loop connecting αE2 and αF2 hydrogen bond with the side chain of Arg 887 (the Arg preceding the PPxY motif) in the bound peptide. Also, Pro 885 and Tyr 886 in β-dystroglycan contact Thr 3188 in this E2F2 loop (Fig. 1*c*). These additional interactions apparently allow dystrophin to distinguish its correct binding site from other PPxY sites in β-dystroglycan and other proteins. Studies of the ligand binding specificity of this region of dystrophin show that a second PPxY motif in β-dystroglycan does not bind to dystrophin within its wild type context (APLPPP**EY**PNQS) but does bind well within the context of the C-terminal peptide studied here (KNMTPYRS**PPEY**VPP). Furthermore, substitutions of Arg 887 to Glu or Asp abolish binding to dystrophin[7]. Thus the EF-hand region serves a dual role; it stabilizes the fold of the WW domain and it provides additional specificity in β-dystroglycan recognition.

We expect that other WW domains that recognize the PPxY motif, including Yap and Nedd4, will bind the motif in the manner that we observe in dystrophin. The residues that line the binding pocket are well-conserved in this class of WW domains (Fig. 2), as are other residues important for defining the conformation of the binding pocket (including Glu 3062, which hydrogen bonds with one nitrogen in the His 3076 side chain, orienting the other imidazole nitrogen for optimal interaction with the hydroxl group of the Tyr in the bound peptide). An NMR and mutagenesis study of the Yap65 WW domain defined a binding surface analogous to the one we observe in dystrophin; however, the mode of PPxY peptide binding modeled in the Yap65 study is different from the one we see in dystrophin[16]. In the Yap NMR model, the position of the peptide relative to the domain is rotated and shifted by 4–5 Å; thus the two prolines in the PPxY sequence do not lie in the aromatic cradle (formed by the residues equivalent to Trp 3083 and Tyr 3072), and no hydrogen bond is formed to the Trp. Also, the PPxY Tyr in the Yap model is oriented differently, such that its side chain extends in a direction perpendicular to that of the corresponding Tyr in our structure. It is possible that the YAP65 WW domain indeed binds the PPxY motif differently, but we believe that the apparent difference is more likely attributable to the modest number of experimental restraints in the NMR study. Ten intermolecular NOEs were measured[16], which may have been insufficient to unambiguously dock the peptide to the surface of the Yap65 domain. Indeed all eight of the ten restraints within the PPPY portion of the peptide would also be satisfied by a binding mode precisely analagous to that in the dystrophin complex (M. Macias, pers. comm.).

Similar proline recognition by WW and SH3 domains

The set of ligand interactions in the dystrophin complex is reminiscent of those observed in other structurally unrelated proline-recognition domains, especially SH3 domains (Fig. 3*b*). In particular, the nature of the contacts with a Trp residue is similar among proline recognition domains. The combination of the stacking of a Pro with the Trp ring and the formation of a hydrogen bond between a carbonyl oxygen in the peptide and the indole nitrogen in the Trp appears to be nearly universal; it is found in SH3 domains[20], EVH1 domains[21,22], and profilin[23] in addition to WW domains. Comparison of the dystrophin structure with that of Pin1 bound to a serine-phosphorylated peptide[24] reveals an additional similarity with SH3 domains, the capacity for 'bidirectional' binding. The Pin1 WW domain binds the phosphoserine peptide using a similar binding surface, but the orientation of the peptide is reversed N-terminal to C-terminal[24]. As with SH3 domains, polarity is in part determined by non-Pro residues (in β-dystroglycan, the Tyr in the

Table 1 Data collection, phasing and refinement statistics

	Dystrophin–β-dystroglycan native	Dystrophin–β-dystroglycan Hg derivative	Unliganded dystrophin native
Wavelength (Å)	1.0332	1.0093	0.9220
Resolution (Å)	1.90	1.90	2.0
Space group	$P2_12_12_1$	$P2_12_12_1$	$P2_12_12_1$
Unit cell (a, b, c; Å)	48.68, 67.05, 83.84	49.13, 67.63, 84.34	49.71, 67.47, 85.49
Molecules per asymmetric unit	1	1	1
R_{sym} (%)	5.2	7.2	5.5
Reflections (total / unique)	120,237 / 21,895	127,542 / 22,527	144,120 / 19,962
Completeness (%)	98.3	98.9	99.2
Phasing power (centric / acentric)		1.27 / 1.66	
R_{cullis} (centric / acentric / anomalous)		0.68 / 0.71 / 0.80	
Figure of merit		0.476	
Number of sites		8	
Refinement statistics			
Resolution range (Å)	20.0–1.9		20.0–2.0
Protein atoms	2,197		2,090
Water molecules	283		266
R_{cryst} / R_{free} (%)	19.7 / 24.9		19.4 / 25.7
R.m.s. deviations			
Bond lengths (Å)	0.013		0.013
Angles (°)	1.654		1.563

PPxY motif and the Arg preceding the motif). Although we expect that dystrophin and other WW domains that recognize the PPxY motif will always bind the motif in the orientation described here, it is possible that they could bind other sequences with the opposite polarity.

The similarity in the binding surfaces of SH3 and WW domains highlights a longstanding question in studies of proline recognition domains — how is specificity achieved? Indeed, some Proline-rich sequences, including the tail of β-dystroglycan, have been observed to bind with both domains[12,25]. The present structure shows how this problem is solved in dystrophin; the WW domain is embedded in a larger module that provides additional binding determinants. Unlike WW domains in many signaling proteins, which likely make ephemeral, low affinity interactions, the dystrophin–dystroglycan complex forms a structural connection between the cytoskeleton and the basal lamina. The additional interactions outside the WW domain, and perhaps further contacts between regions of dystrophin and β-dystroglycan not present in the fragments studied here, may provide the affinity and structural rigidity required in such a component of a force-generating contractile cell.

Methods

Purification and crystallization. The DBR region of human dystrophin (residues 3046–3306) was expressed in *Escherichia coli* strain BL21 using the expression plasmid pGEX2TK (Pharmacia). Cell pellets were lysed by sonication in 50 mM Tris pH 8.0, 150 mM NaCl, 5 mM dithiothreitol, and 1 mM PMSF (phenylmethylsulfonyl fluoride). The pH of the cleared lysate was lowered by the addition of 50 mM MOPS (3-[N-morpholino]propanesulfonic acid) pH 6.5 before incubation with glutathione-agarose beads. After an extensive wash with 50 mM MOPS pH 6.5, 100 mM NaCl, 5 mM DTT, the dystrophin protein was cleaved from the beads with thrombin, and further purified by cation exchange chromatography (S-Sepharose FF, Pharmacia). The purified protein was concentrated to 10 mg ml^{-1} in storage buffer (20 mM MOPS pH 6.5, 100 mM NaCl, and 5 mM DTT). The purified dystrophin protein contained an additional nine residues (GSRRASVGS) from the glutathione-S-transferase (GST) fusion.

All dystrophin crystals were grown in hanging drops at 22 °C by combining 2.5 μl of protein in storage buffer with 2.5 μl of a well solution. The unliganded crystals were grown with a well solution containing 100 mM MOPS pH 6.5, 1.0 M ammonium sulfate, 10% glycerol (v/v), and 5 mM DTT. For cocrystallization with the β-dystroglycan peptide (residues 881–885, KNMTPYRSPPPYVPP) a 3–6 fold molar excess of peptide was added to the dystrophin protein in storage buffer. The complex was crystallized over a well solution containing 100 mM Hepes pH 7.0, 1.0 M ammonium sulfate, 10% glycerol (v/v), and 5 mM DTT.

Data collection, structure determination and refinement. All crystals were transferred to stabilizing solutions containing the components of their respective crystallization buffers and at least 20% glycerol (v/v). The mercury derivative was prepared by soaking a complex crystal overnight in stabilizing solution containing 1.0 mM methyl mercury nitrate and no DTT. All diffraction data were recorded at 100 K. Unit cell constants and other structure determination statistics for all crystal forms are given in Table 1. Diffraction data for the complex crystals were recorded using a 3×3 mosaic CCD detector at the Structural Biology Center's undulator beamline 19ID at the Advanced Photon Source, Argonne National Laboratory. The mercury derivative was collected at the mercury LIII edge as determined by an X-ray fluorescence scan. Diffraction data for the unliganded crystals were recorded using ADSC Quantum-4 CCD detector on the F1 beam line at the Cornell High Energy Synchrotron Source (CHESS). All data were collected in a single pass using a 1° oscillation. Diffraction data were integrated and scaled using the programs DENZO and SCALEPACK[26].

The structure of the complex was determined by SIRAS (single isomorphous replacement with anomalous scattering) using a methyl mercury nitrate derivative. Eight mercury sites were located by using difference Patterson and difference Fourier methods using the CCP4 program suite[27] and the program PATSOL[28]. Structure factor phases were calculated using MLPHARE[29] and improved with solvent flattening and histogram matching using DM[27]. The resulting electron density map was readily interpretable. With the aid of skeletonization using BONES[30], a nearly complete model of dystrophin (residues 3048–3065, 3069–3165, 3170–3304) was built using the molecular graphics program O[30]. After an initial round of crystallographic refinement using X-PLOR[31], the electron density map was further improved using ARP/wARP[32]. The remaining residues of dystrophin and β-dystroglycan peptide were then built; the final model includes residues 3047–3306 of dystrophin and residues 882–894 of β-dystroglycan peptide. The complete model was further refined using simulated annealing and positional refinement in

X-PLOR[31], and water molecules were added with ARP/wARP[32]. Tightly restrained individual B-factors were refined and a bulk-solvent model was incorporated. Crystallographic R-factors and stereochemical parameters are presented in Table 1.

The unliganded dystrophin crystals were nearly isomorphous with those of the complex. The complex structure (with β-dystroglycan peptide removed) was used as an initial model. After rigid body refinement using X-PLOR[31], rebuilding and refinement of the unliganded structure was carried out as described above for the complex. The final model includes residues 3047–3306 of dystrophin (Table 1).

Coordinates. Coordinates and structure factors have been deposited in the Protein Data Bank (accession codes 1EG3 and 1EG4 for the free and complex structures, respectively).

Acknowledgments

The authors thank C. Dahl for synthesis and purification of the β-dystroglycan peptide and A. Farooq for help with microcalorimetry measurements. We thank M. Macias for coordinates of the Yap WW domain and for helpful discussions in comparing the structures. This work was supported in part by grants from the NIH (to M.S.), the Muscular Dystrophy Association (to M.J.E. and M.S.), and by the US Department of Energy, Office of Biological and Environmental Research (to A.J. and Rg.Z). M.J.E. is a recipient of a Burroughs-Wellcome Career award in the Biomedical Sciences, and a member of the Harvard-Armenise Center for Structural Biology. Diffraction data were recorded at the Advanced Photon Source at Argonne National Labs, and at CHESS, which is supported by grants from the NIH and NSF.

Correspondence should be addressed to M.J.E. *email: eck@red.dfci.harvard.edu*

Received 25 April, 2000; accepted 30 June, 2000.

1. Koenig, M., Monaco, A.P. & Kunkel, L.M. *Cell* **53**, 219–226 (1988).
2. Straub, V. & Campbell, K.P. *Curr. Opin. Neurol.* **10**, 168–175 (1997).
3. Tinsley, J.M., Blake, D.J., Zuellig, R.A. & Davies, K.E. *Proc. Natl. Acad. Sci. USA* **91**, 8307–8313 (1994).
4. Koenig, M. *et al. Am. J. Hum. Genet.* **45**, 498–506 (1989).
5. Roberts, R.G., Bobrow, M. & Bentley, D.R. *Proc. Natl. Acad. Sci. USA* **89**, 2331–2335 (1992).
6. Jung, D., Yang, B., Meyer, J., Chamberlain, J.S. & Campbell, K.P. *J. Biol. Chem.* **270**, 27305–27310 (1995).
7. Rentschler, S. *et al. Biol. Chem.* **380**, 431–442 (1999).
8. Sudol, M. *Prog. Biophys. Mol. Biol.* **65**, 113–132 (1996).
9. Kay, B.K., Williamson, M.P. & Sudol, M. *FASEB J.* **14**, 231–241 (2000).
10. Komuro, A., Saeki, M. & Kato, S. *J Biol Chem* **274**, 36513–36519 (1999).
11. Chen, H.I. & Sudol, M. *Proc. Natl. Acad. Sci. USA* **92**, 7819–7823 (1995).
12. Bedford, M.T., Chan, D.C. & Leder, P. *EMBO J.* **16**, 2376–2383 (1997).
13. Bedford, M.T., Reed, R. & Leder, P. *Proc. Natl. Acad. Sci. USA* **95**, 10602–10607 (1998).
14. Lu, P.J., Zhou, X.Z., Shen, M. & Lu, K.P. *Science* **283**, 1325–1328 (1999).
15. Ranganathan, R., Lu, K.P., Hunter, T. & Noel, J.P. *Cell* **89**, 875–886 (1997).
16. Macias, M.J. *et al. Nature* **382**, 646–649 (1996).
17. Ikura, M. *Trends Biochem. Sci.* **21**, 14–17 (1996).
18. de Beer, T., Carter, R.E., Lobel-Rice, K.E., Sorkin, A. & Overduin, M. *Science* **281**, 1357–1360 (1998).
19. Meng, W., Sawasdikosol, S., Burakoff, S.J. & Eck, M.J. *Nature* **398**, 84–90 (1999).
20. Musacchio, A., Saraste, M. & Wilmanns, M. *Nature Struct. Biol.* **1**, 546–551 (1994).
21. Prehoda, K.E., Lee, D.J. & Lim, W.A. *Cell* **97**, 471–480 (1999).
22. Fedorov, A.A., Fedorov, E., Gertler, F. & Almo, S.C. *Nature Struct. Biol.* **6**, 661–665 (1999).
23. Mahoney, N.M., Rozwarski, D.A., Fedorov, E., Fedorov, A.A. & Almo, S.C. *Nature Struct. Biol.* **6**, 666–671 (1999).
24. Verdecia, M.A., Bowman, M.E., Lu, K.P., Hunter, T. & Noel, J.P. *Nature Struct. Biol.* **7**, 639-643 (2000).
25. Yang, B. *et al. J. Biol. Chem.* **270**, 11711–11714 (1995).
26. Otwinowski, Z. & Minor, W. *Methods Enzymol.* **276**, 307–326 (1997).
27. Collaborative Computational Project Number4. *Acta Crystallogr. D* **50**, 760–776 (1994).
28. Tong, L. & Rossman, M.G. *J. Appl. Crystallogr.* **26**, 15–21 (1993).
29. Otwinowski, Z. in *Isomorphous replacement and anomalous scattering*, Proc. Daresbury Study Weekend, 80–85 (SERC Daresbury Laboratory, Warrington, UK; 1991)
30. Jones, T.A. & Kjeldgaard, M. *Methods Enzymol.* **277**, 173–208 (1997).
31. Brunger, A. *X-PLOR Version 3.0: a system for crystallography and NMR.* (Yale University Press, New Haven; 1992).
32. Lamzin, V.S. & Wilson, K.S. *Methods Enzymol.* **277**, 269–305 (1997).
33. Nguyen, J.T., Turck, C.W., Cohen, F.E., Zuckermann, R.N. & Lim, W.A. *Science* **282**, 2088–2092 (1998).